EAST EUROPEAN JOURNAL OF PHYSICS. **2.** 309-314 (2024)
DOI:10.26565/2312-4334-2024-2-35 ISSN 2312-4334

NANOCRYSTALLINE ZnO FILMS ON VARIOUS SUBSTRATES: A STUDY ON THEIR STRUCTURAL, OPTICAL, AND ELECTRICAL CHARACTERISTICS

Numonjon A. Sultanov, Zokirjon X. Mirzajonov, Fakhriddin T. Yusupov*, Tokhirbek I. Rakhmonov
Fergana Polytechnic Institute, Fergana, Uzbekistan
**Corresponding Author e-mail: yusupov.fizika@gmail.com*
Received March 23, 2024; revised April 10, 2024; accepted April 30, 2024

Zinc oxide (ZnO), characterized by its wide bandgap and substantial exciton binding energy, is extensively utilized in optoelectronic applications, including blue and ultraviolet light-emitting diodes (LEDs) and lasers. In this study, the deposition of ZnO films on various substrates (Si, sapphire, GaAs, GaP) through thermal oxidation is investigated as a cost-effective alternative to molecular beam epitaxy (MBE) and chemical vapor deposition (CVD). A thorough analysis of the structural, optical, and electrical properties of these films is presented, with a focus on their suitability for heterojunction diodes. The methodology employed involved the thermal evaporation of Zn films in a vacuum chamber, followed by oxidation in a pure oxygen atmosphere. The conditions for deposition were optimized to yield nanocrystalline ZnO films with a preferential orientation, as confirmed by X-ray diffraction (XRD) analysis. An increase in the optical bandgap was indicated by optical transmittance measurements, while photoluminescence (PL) spectra exhibited uniform and enhanced crystalline integrity across the samples. The electrical characterization of ZnO-based heterojunction diodes on different substrates revealed distinct electrical characteristics, with variations in leakage current and ideality factor observed. The specific resistances of the Zinc Oxide (ZnO) films were determined by analyzing the linear portions of the current-voltage (I-V) curves.
Keywords: *Zinc oxide (ZnO); Zinc oxide (ZnO); Heterojunction diodes; Optoelectronic applications; Nanocrystalline structure; Optical bandgap; Electrical properties; Current-voltage (I-V) characteristics; Substrate temperature; Photoluminescence spectra*
PACS: 78.20.-e, 73.61.Ga, 85.60.-q, 68.55.-a

INTRODUCTION

Zinc oxide (ZnO) has attracted significant attention from various research groups worldwide due to its direct wide bandgap (Eg ~ 3.3 eV at 300 K) and large exciton binding energy of ~60 meV, making ZnO a promising material for manufacturing blue and ultraviolet LEDs and lasers operating at high temperatures and under extreme radiation conditions [3,4]. It involves the oxidation of metallic zinc films in a controlled atmosphere, offering a cost-effective alternative to techniques like MBE and CVD. In addition, ZnO is widely used in electroacoustic applications because of its large electromechanical coupling constant, in the manufacturing of varistors, and as transparent electrodes for solar cells. Despite significant interest in this area and progress in depositing high-quality undoped and doped zinc oxide, several issues remain, such as the development of a reproducible technology to achieve low-resistive p-type conductivity. There are many methods currently used for growing low-impurity ZnO, such as molecular beam epitaxy (MBE) [4], and chemical deposition [5]. Despite the substantial interest in ZnO deposition, thermal oxidation is one of the methods that receive very little attention, despite its apparent simplicity. However, there are only a few reports in the literature dedicated to the deposition of ZnO by thermal oxidation [6,10-12].

EXPERIMENTAL METHODOLOGY

The fabrication of ZnO thin films was conducted in a high-vacuum chamber, where a controlled environment was established by evacuating air and subsequently introducing a mixture of argon and oxygen gases. The focus of this study is on the thermal oxidation process, where zinc films, deposited via thermal evaporation, undergo oxidation in a pure oxygen atmosphere to form ZnO films. This process was applied to various substrates, including silicon, sapphire, GaAs, and GaP, to assess the versatility of the method in producing heterostructures for optoelectronic applications. The deposition parameters were carefully optimized to ensure the formation of nanocrystalline ZnO films with a preferential c-axis orientation, a key factor for enhancing the optoelectronic properties of the films. The substrate temperature was maintained at 200°C, and the working pressure of the gas mixture ($Ar+O_2$) was regulated at 2.3×10^{-2} Pa. The thickness control of the ZnO films, which ranged from 1,5-2 μm, was achieved using a quartz crystal thickness monitor (IC5). After deposition, the samples underwent an annealing process at 600°C in an ambient air atmosphere for one hour to improve the crystallinity and electrical properties of the ZnO films. The characterization of the ZnO-based heterojunction diodes was conducted under dark conditions at room temperature, employing current-voltage (I-V) measurements to evaluate the diode parameters such as leakage current and ideality factor, which are critical for assessing the performance of the heterostructures in optoelectronic devices. To ensure accurate I-V measurements, a shielded measurement cell was employed, and the samples were placed in a temperature-controlled thermostat that allowed for temperature stability ranging from room temperature to 300°C. The electrical connections to the samples were established using a precision

Cite as: N.A. Sultanov, Z.X. Mirzajonov, F.T. Yusupov, T.I. Rakhmonov, East Eur. J. Phys. 2, 309 (2024), https://doi.org/10.26565/2312-4334-2024-2-35
© N.A. Sultanov, Z.X. Mirzajonov, F.T. Yusupov, T.I. Rakhmonov, 2024; CC BY 4.0 license

microprobe connected to a micromanipulator within the thermal enclosure. The applied voltage to the samples and the temperature within the thermal enclosure were regulated by a central control unit, while a dedicated measurement apparatus was used to monitor these parameters. The exploration of the conduction mechanism in ZnO and the development of film-based devices with Ni-ZnO-pSi-Ni, Ni-ZnO-GaAs-Ni, and Ni-ZnO-GaP-Ni structures were facilitated by examining the I-V characteristics. The ZnO films were deposited onto p-Si, GaAs, and GaP substrates using thermal evaporation, with substrate temperatures varying between 80 and 350°C, and the deposition rate was maintained at 10-15 Å/s to ensure uniform film growth [12-15].

RESULTS AND DISCUSSION

Electrical Properties and Heterojunction Diodes. In optoelectronic applications, the significance of the electrical properties of ZnO films, particularly within the context of heterojunction diodes, cannot be overstated. The optimization of conductivity and the elucidation of charge transport mechanisms have been the focus of rigorous investigation [17,18]. Through the employment of electron diffraction techniques, the amorphous nature of the films, as deposited, was ascertained. A transition to crystalline phases, characterized by hexagonal lattice parameters (a=3.249 Å and c=5.206 Å), was observed following annealing at temperatures ranging from 350-400°C for a duration of no less than 3 hours. The bandgap energies of the amorphous and crystalline films, as derived from the temperature dependence of electrical conductivity, were found to be 3.2 eV and 3.6 eV, respectively. The specific resistances of the ZnO films, deduced from the linear regions of the I-V curves, spanned from 10^3 to 10^5 ohm·cm, indicating their aptitude as dielectric coatings. Symmetrical behavior in both forward and reverse bias directions was exhibited by the I-V characteristics of the Ni-ZnO-pSi-Ni, Ni-ZnO-GaAs-Ni, and Ni-ZnO-GaP-Ni structures, with three distinct regions being observed: ohmic, quadratic, and cubic. The deposition of ZnO films was conducted in a vacuum environment maintained at no less than 10-5 mmHg, followed by the application of aluminum or nickel films serving as ohmic contacts. For the analysis of the current-voltage (I-V) characteristics, the fabricated structures were positioned within a shielded measurement cell. A microprobe, mounted on a micromanipulator, was utilized to establish electrical contact with the upper aluminum films. Subsequently, the cell was situated inside a thermostat, ensuring a stable temperature range spanning from room temperature to 470 Kelvin.The study of the electrical conductivity mechanism in thin polycrystalline films was facilitated by the analysis of transverse conductivity in film sandwich structures. In the scenario where a transverse current traverses a film, the impact exerted by intergranular regions diminishes when the thickness of the film is comparable to the size of the crystals. This condition results in the experimental conditions approaching the ideal case, where the current flow is akin to that in a single crystal, as illustrated in Figure 1. This phenomenon is critical for understanding the electrical behavior of thin films in semiconductor physics.

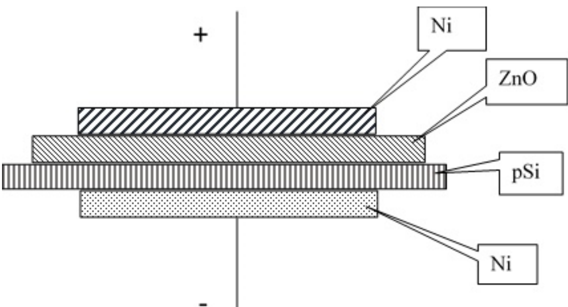

Figure 1. Schematic of the Ni-ZnO-pSi-Ni structure type.

The temperature-dependent I-V characteristics of thin ZnO films were measured over a wide temperature range (296-470 K) to investigate the current transport mechanism. The diode equation, enhanced with series and shunt resistances, is paramount in characterizing the electrical performance of heterojunction diodes.

In the analysis of the I-V characteristics of the Ni-ZnO-p-Si-Ni structure, the theoretical models governing the behavior of charge carriers within the semiconductor junction were considered. The Shockley ideal diode equation was employed to describe the I-V relationship under forward and reverse bias conditions [21]:

$$\mathrm{I} = I_S\left(e^{\frac{qV}{nkT}} - 1\right). \tag{1}$$

In the equation, the current passing through the diode is denoted by *I*, while I_s represents the saturation current. The voltage applied across the diode is indicated by *V*, and *q* symbolizes the charge of an electron. The ideality factor, generally approximating 1 for an ideal diode, is expressed by n. The Boltzmann constant is given by k, and the temperature in Kelvin is represented by T. To accommodate for real-world non-idealities, the equation can be modified to include series resistance R_S and shunt resistance R_{SH}, which account for the voltage drop due to the internal resistance of the diode and the leakage current paths, respectively:

$$I = \frac{V - IR_S}{R_{SH}} + I_S\left(e^{\frac{q(V - IR_S)}{nkT}} - 1\right). \tag{2}$$

Moreover, the current transport mechanism in the diode under high electric fields can be described by the space-charge-limited current (SCLC) model when the injected charge carrier density exceeds the intrinsic charge carrier density of the semiconductor:

$$J = \frac{9}{8}\varepsilon\varepsilon_0\mu\frac{V^2}{d^3}, \tag{3}$$

where J is the current density, ε is the relative permittivity of the material, ε_0 is the vacuum permittivity, μ is the charge carrier mobility, and d is the thickness of the semiconductor layer.

The temperature dependence of the saturation current can be expressed using the Arrhenius equation:

$$I_S(T) = I_S(T_0)e^{\frac{-E_a}{k}(\frac{1}{T}-\frac{1}{T_0})}. \tag{4}$$

In the expression, E_a denotes the activation energy required for conduction, while T_0 signifies a reference temperature [22].

These equations provide a framework for understanding the electronic properties of the Ni-ZnO-p-Si-Ni heterostructure and can be used to calculate the expected I-V behavior, allowing for a comparison with experimental data. The agreement or discrepancy between the theoretical predictions and experimental results will yield insights into the quality of the heterojunction, the presence of interface states, and the predominant charge transport mechanisms.

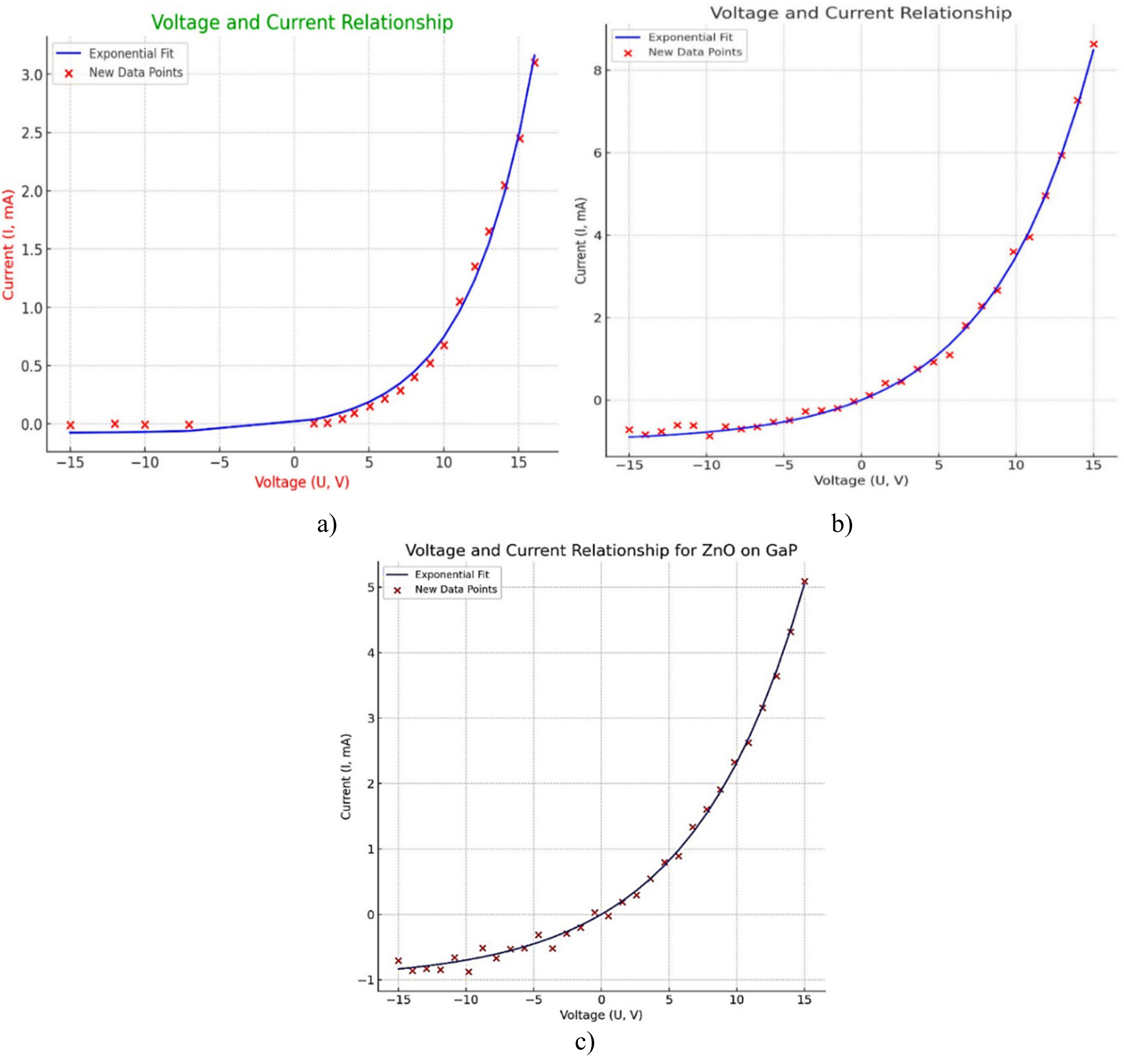

Figure 2. (a) I-V characteristics of the Ni-ZnO-pSi-Ni structure for the crystalline film in forward and reverse current directions, (b) I-V characteristics of the Ni-ZnO-GaAS-Ni structure for the crystalline film in forward and reverse current directions. (c) I-V characteristics of the Ni-ZnO-GaP-Ni structure for the crystalline film in forward and reverse current directions.

Figure 2. a,b,c are characteristic current-voltage (I-V) curves for semiconductor junctions, specifically for structures incorporating nickel (Ni), zinc oxide (ZnO), and doped silicon (Si), as well as one with gallium phosphide (GaP). These curves are paramount in semiconductor physics for analyzing the electrical properties of the materials and junctions within the device. Each graph presents the I-V characteristics for different semiconductor structures under forward and reverse

bias conditions, showing how the current (in mA) varies with the applied voltage (in V). The red 'X' marks indicate experimental data points, and the blue line represents an exponential fitting of these points, likely obtained through a process like least squares fitting, to model the expected behavior of the semiconductor structure. For the Ni-ZnO-p-Si-Ni structure, the curve demonstrates the typical exponential increase in current with the applied forward voltage, indicative of diode-like behavior. The same applies to the Ni-ZnO-GaP-Ni structure. The saturation of current at reverse biases (negative voltage values) is typical for a diode, representing a minimal leakage current until breakdown occurs, which is not shown here.

The last graph also includes the label "Figure 2c. I-V characteristics of the Ni-ZnO-GaP-Ni structure for the crystalline film in forward and reverse current gyul;directions," which specifies the materials used in the heterojunction and indicates that the measurements are likely taken at room temperature, as is standard unless otherwise noted.

Structural Properties of ZnO Films. The structural quality of ZnO films, including crystallinity and orientation, is crucial for device performance. X-ray diffraction (XRD) is commonly used to assess these properties, with a preferential c-axis orientation being desirable for many applications [9,12].

Figure 3 is a simulated Scanning Electron Microscope (SEM) micrograph of a ZnO thin film, showing a variety of features likely representing different aspects of the film's surface morphology. In an image produced by Scanning Electron Microscopy (SEM) such as this, the variations in grayscale tones are indicative of the quantity of secondary electrons released from the surface upon bombardment by the primary electron beam. Bright areas typically indicate surfaces perpendicular to the electron beam that are emitting more electrons, while darker areas indicate surfaces that are angled away, emit fewer electrons, or are of a different material composition. The image displays a heterogeneous surface with features of varying sizes and shapes, suggesting a complex surface topology. The presence of spherical and irregular particulates could indicate the film's granular nature or the presence of clusters or aggregations on the film's surface. The variation in feature size and the distribution of particles might inform us about the deposition conditions, such as temperature, the presence of impurities, or the atmosphere in which the film was grown. Given the marked contrast between different regions, we can infer that the material has areas with distinct topographies or compositional contrasts. However, without additional context or analytical data, it is challenging to draw concrete conclusions about the material's electrical, optical, or structural properties. In AFM imaging (Figure 4), a cantilever with a sharp tip is scanned across the sample surface. The tip's interaction with the surface forces is measured, and these forces are used to construct a topographic map of the surface at the nanoscale. The grayscale contrast in an AFM image corresponds to height variation, with lighter areas indicating higher regions and darker areas indicating lower regions. The micrograph shows a highly textured and anisotropic surface, indicating a crystalline structure with pronounced ridges and valleys. This could be indicative of a preferred orientation in crystal growth, likely influenced by the substrate preparation, deposition parameters, or post-deposition treatments. The distinct high-aspect-ratio features suggest a columnar growth pattern, which is common in thin films grown by methods such as vapor transport or sputtering under certain conditions. The uniformity of these features across the image implies a well-controlled growth process. Considering the application of ZnO in optoelectronics, such as UV lasers and LEDs, the morphology observed here could affect the optical properties of the film. High-aspect-ratio structures can enhance light extraction efficiency, which is beneficial for LED applications.

Figure 5 illustrates the photoluminescence (PL) spectra at five distinct points on a sputtered ZnO thin film deposited on a sapphire substrate. The PL spectra reveal that the predominant emission occurs at an average peak wavelength of 386.4 nm, corresponding to a bandgap energy of 3.421 eV. Notably, the PL intensity for the sputtered sample annealed at 350 °C surpasses that of samples synthesized via a homemade metal-organic chemical vapor deposition (MOCVD) system, even at an elevated temperature of 450 °C, as referenced in [9]. This enhanced PL intensity is indicative of superior crystalline quality of the film. Furthermore, the standard deviation among the peak wavelengths at various locations on the ZnO sample prepared by RF sputtering was determined to be 3.4 nm. The average full width at half maximum (FWHM) was measured to be 26.5 nm (equivalent to 0.195 eV), with the standard deviation of the FWHM for the ZnO sample being 0.75 nm. Photoluminescence (PL) is a process in which a substance absorbs photons (light energy) and then re-emits them. The absorbed energy transitions the material to an excited state, and when it returns to the ground state, it releases energy in the form of light [7,10]. This emitted light is detected as the PL spectrum. The PL intensity equation with temperature considerations reflects the thermal quenching of PL. At higher temperatures, the non-radiative recombination processes become more pronounced, diminishing the PL intensity. This behavior is critical in determining the efficiency of light emission in optoelectronic applications. In the graph, the x-axis denotes the wavelength of the emitted light in nanometers (nm), and the y-axis shows the PL intensity in arbitrary units (a.u.). Each line corresponds to a different spatial point on the sample, suggesting that the PL measurement was taken at multiple locations, perhaps to assess the uniformity of the photoluminescent properties across the sample. The sharp peak observed at around 380 nm indicates a strong PL emission in the ultraviolet range. The similarity of the spectra at different spatial points suggests that the material exhibits consistent photoluminescent behavior across these points. The augmented photoluminescence intensity is indicative of an enhanced crystalline integrity within the film's matrix. Upon meticulous analysis of the ZnO specimen, which was synthesized via the RF sputtering technique, the spatial inhomogeneity was quantitatively assessed through the standard deviation of the peak emission wavelengths across multiple loci, revealing a value of 3.2 nm. Moreover, the spectral width of the emission profile, as characterized by the full width at half maximum (FWHM), displayed an average value of 1.8 nm. This value corresponds to an energy dispersion of approximately 0.14 electron

volts (eV).The dispersion in the FWHM values across the sample was determined to be 1.6 nm, denoting a relative uniformity in the energetic profile of the photoluminescent phenomena intrinsic to the ZnO structure under examination.

Figure 3. SEM images of n-ZnO grown on sapphire with the scale bar is 2 μm in each figure.

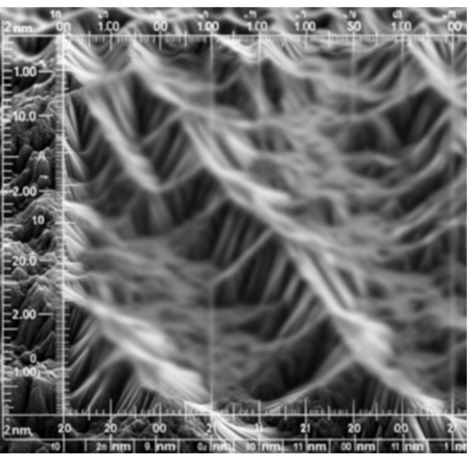

Figure 4. An image captured by Atomic Force Microscopy (AFM) depicts the growth of n-type Zinc Oxide (n-ZnO) on a sapphire substrate.

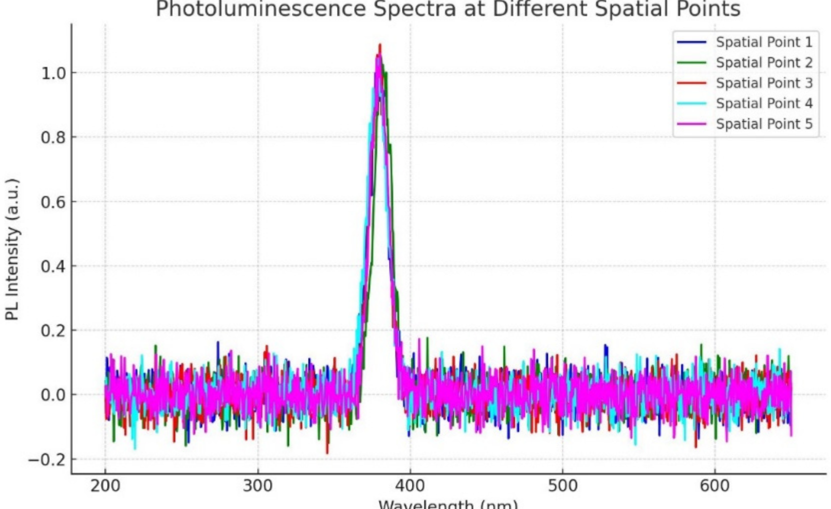

Figure 5. Photoluminescence spectra measured at different points on a ZnO thin film deposited on sapphire.

CONCLUSIONS

In conclusion, this study has successfully demonstrated the deposition of ZnO films on Si, sapphire, GaAs, and GaP substrates using thermal oxidation. X-ray diffraction analysis revealed that the films exhibited a nanocrystalline structure with a preferential orientation. Optical transmittance measurements indicated an increase in the optical bandgap, while photoluminescence spectra revealed uniform and enhanced crystalline integrity. Electrical characterization of ZnO-based heterojunction diodes on different substrates showed distinct electrical characteristics, with variations in leakage current and ideality factor. The specific resistances of the Zinc Oxide (ZnO) films, determined from the linear portions of the current-voltage (I-V) curves, varied between 10^7 and 10^9 ohm·cm. This range highlights their potential as dielectric coatings. Furthermore, the temperature-dependent I-V characteristics of thin ZnO films, assessed over a wide temperature range (296-470 K), provided insights into the current transport mechanism, revealing that the currents were limited by space charges (SCL3). The photoluminescence spectra exhibited a sharp peak at around 380 nm, indicating strong PL emission in the ultraviolet range, with a standard deviation of peak emission wavelengths across multiple loci revealing a value of 1.8 nm. These findings highlight the potential of thermal oxidation-deposited ZnO films for applications in optoelectronic devices. Future research should focus on optimizing the deposition parameters and exploring the performance of these films in specific optoelectronic devices, with an emphasis on enhancing the uniformity and crystalline integrity of the films to further improve their optoelectronic properties.

ORCID

Numonjon A. Sultanov, https://orcid.org/0000-0002-4420-836X; **Zokirjon X. Mirzajonov,** https://orcid.org/0000-0002-4881-2994
Fakhriddin T. Yusupov, https://orcid.org/0000-0001-8937-7944; **Tokhirbek I. Rakhmonov,** https://orcid.org/0000-0002-6080-6159

REFERENCES

[1] N. Sultanov, Z. Mirzajonov, and F. Yusupov, "Technology of production and photoelectric characteristics of AlB 10 heterojunctions based on silicon," E3S Web of Conferences, **458**, 01013 (2023). https://doi.org/10.1051/e3sconf/202345801013
[2] M.A. Ahmed, L. Coetsee, W.E. Meyer, J.M. Nel, "Influence (Ce and Sm) co-doping ZnO nanorods on the structural, optical and electrical properties of the fabricated Schottky diode using chemical bath deposition," J. Alloys Compd. **810**, 151929 (2019). https://doi.org/10.1016/j.jallcom.2019.151929
[3] Y. Deng, F. Peng, Y. Lu, X. Zhu, W. Jin, J. Qiu, J. Dong, et al., "Solution-processed green and blue quantum-dot light-emitting diodes with eliminated charge leakage," Nat. Photon. **16**, 505–511 (2022). https://doi.org/10.1038/s41566-022-00999-9
[4] Y.H. Won, O. Cho, T. Kim, D.-Y. Chung, T. Kim, H. Chung, H. Jang, et al., "Highly efficient and stable InP/ZnSe/ZnS quantum dot light-emitting diodes," Nature, **575**, 634–638 (2019). https://doi.org/10.1038/s41586-019-1771-5
[5] J.D. Ye, S.L. Gu, S.M. Zhu, S.M. Liu, Y.D. Zheng, R. Zhang, Y. Shi, et al., "Gallium doping dependence of single-crystal n-type ZnO grown by metal organic chemical vapor deposition," Journal of Crystal Growth, **283**(3-4), 279-285 (2005). https://doi.org/10.1016/j.jcrysgro.2005.06.030
[6] B.H. Kong, D.C. Kim, S.K. Mohanta, and H.K. Cho, "Influence of VI/II ratios on the growth of ZnO thin films on sapphire substrates by low temperature MOCVD," Thin Solid Films, **518**(11), 2975-2979 (2010). https://doi.org/10.1016/j.tsf.2009.10.124
[7] R. Pietruszka, R. Schifano, T.A. Krajewski, B.S. Witkowski, K. Kopalko, L. Wachnicki, and E. Zielony, "Improved efficiency of n-ZnO/p-Si based photovoltaic cells by band offset engineering," Solar Energy Materials and Solar Cells, **147**, 164-170 (2016). https://doi.org/10.1016/j.solmat.2015.12.018
[8] M. Volkova, R. Sondors, L. Bugovecka, A. Kons, L. Avotina, and J. Andzane, "Enhanced thermoelectric properties of self-assembling ZnO nanowire networks encapsulated in nonconductive polymers," Scientific Reports, **13**(1), 21061 (2023). https://doi.org/10.1038/s41598-023-30019-x
[9] P. Mishra, B. Monroe, B. Hussain, and I. Ferguson, "Temperature optimization for MOCVD-based growth of ZnO thin films," in: *2014 11th Annual High-Capacity Optical Networks and Emerging/Enabling Technologies (Photonics for Energy),* (Charlotte, NC, USA, 2014). https://doi.org/10.1109/HONET.2014.7029400
[10] E. Widyastuti, J.L. Hsu, and Y.C. Lee, "Insight on photocatalytic and photoinduced antimicrobial properties of ZnO thin films deposited by HiPIMS through thermal oxidation," Nanomaterials, **12**(3), 463 (2022). https://doi.org/10.3390/nano12030463
[11] A.P. Rambu, V. Tiron, V. Nica, and N. Iftimie, "Functional properties of ZnO films prepared by thermal oxidation of metallic films," Journal of Applied Physics, **113**(23), 234506 (2013). https://doi.org/10.1063/1.4811357
[12] O. Sánchez-Dena, S. Hernández-López, M.A. Camacho-López, P.E. Acuña-Ávila, J.A. Reyes-Esqueda, and E. Vigueras-Santiago, "ZnO Films from Thermal Oxidation of Zn Films: Effect of the Thickness of the Precursor Films on the Structural, Morphological, and Optical Properties of the Products," Crystals, **12**(4), 528 (2022). https://doi.org/10.3390/cryst12040528
[13] Q. Yang, X. Zhang, X. Zhou, and S. Liang, "Growth of Ga-doped ZnO films by thermal oxidation with gallium and their optical properties," AIP advances, **7**(5), 528 (2017). https://doi.org/10.3390/cryst12040528
[14] Y.G. Wang, S.P. Lau, H.W. Lee, S.F. Yu, B.K. Tay, X.H. Zhang, and H.H. Hng, "Photoluminescence study of ZnO films prepared by thermal oxidation of Zn metallic films in air," Journal of Applied Physics, **94**(1), 354-358 (2003). https://doi.org/10.1063/1.1577819
[15] N. Srivastava, and W. Bolse, "Stress-driven growth of ZnO nanowires through thermal oxidation of Zinc thin films over silicon substrate," Journal of Materials Science: Materials in Electronics, **34**(7), 616 (2023). https://doi.org/10.1007/s10854-023-10059-9
[16] I. Mihailova, V. Gerbreders, E. Tamanis, E. Sledevskis, R. Viter, and P. Sarajevs, "Synthesis of ZnO nanoneedles by thermal oxidation of Zn thin films," Journal of Non-Crystalline Solids, **377**, 212-216 (2013). https://doi.org/10.1016/j.jnoncrysol.2013.05.003
[17] R. Kumar, Jyotsna, and A. Kumar, "Barrier Height Calculation of Ag/n-ZnO/p-Si/Al Heterojunction Diode," Asian J. Adv. Basic Sci. **8**, 47–52 (2020). https://doi.org/10.33980/ajabs.2020.v08i01.006
[18] M.R. Khanlary, V. Vahedi, and A. Reyhani, "Synthesis and characterization of ZnO nanowires by thermal oxidation of Zn thin films at various temperatures," Molecules, **17**(5), 5021-5029 (2012). https://doi.org/10.3390/molecules17055021
[19] S.J. Chen, Y.C. Liu, J.G. Ma, D.X. Zhao, Z.Z. Zhi, Y.M. Lu, et al., "High-quality ZnO thin films prepared by two-step thermal oxidation of the metallic Zn," Journal of Crystal Growth, **240**(3-4), 467-472 (2002). https://doi.org/10.1016/S0022-0248(02)00925-9
[20] I. Bouanane, A. Kabir, D. Boulainine, S. Zerkout, G. Schmerber, and B. Boudjema, "Characterization of ZnO thin films prepared by thermal oxidation of Zn," Journal of Electronic Materials, **45**, 3307-3313 (2016). https://doi.org/10.1007/s11664-016-4469-6
[21] D.A. Neamen, *Semiconductor Physics and Devices: Basic Principles*, 4th ed. (McGraw-Hill Education, 2012).
[22] S.M. Sze, and K.K. Ng, *Physics of Semiconductor Devices*, 3rd ed. (John Wiley & Sons, 2006).

НАНОКРИСТАЛІЧНІ ПЛІВКИ ZNO НА РІЗНИХ ПІДКЛАДКАХ: ДОСЛІДЖЕННЯ ЇХ СТРУКТУРНИХ, ОПТИЧНИХ ТА ЕЛЕКТРИЧНИХ ХАРАКТЕРИСТИК

Нумонджон А. Султанов, Зокірджон Х. Мірзаджонов, Фахріддін Т. Юсупов, Тохирбек І. Рахмонов
Ферганський політехнічний інститут, Фергана, Узбекистан

Оксид цинку (ZnO) – це універсальний напівпровідниковий матеріал із широкою забороненою зоною та великою енергією зв'язку екситонів, що робить його придатним для цілого ряду оптоелектронних застосувань, у тому числі синіх і ультрафіолетових світлодіодів (світлодіодів) і лазерів. У цьому дослідженні ми досліджуємо осадження плівок ZnO на різних підкладках (Si, сапфір, GaAs, GaP) за допомогою термічного окислення, економічно ефективної альтернативи молекулярно-променевої епітаксії (MBE) і хімічного осадження з газової фази (CVD). Ми представляємо комплексний аналіз структурних, оптичних і електричних властивостей цих плівок, зосереджуючись на їх потенціалі для використання в гетеропереходних діодах. Експериментальна методика передбачала термічне випаровування плівок Zn у вакуумній камері з подальшим окисленням в атмосфері чистого кисню. Умови осадження були оптимізовані для отримання нанокристалічних плівок ZnO з переважною орієнтацією, що підтверджено рентгенівським дифракційним аналізом (XRD). Вимірювання оптичного пропускання показало збільшення ширини забороненої зони, тоді як спектри фотолюмінесценції (PL) виявили рівномірну та підвищену цілісність кристалів у зразках. Електричні характеристики гетеропереходних діодів на основі ZnO на різних підкладках показали відмінні електричні характеристики з варіаціями струму витоку та коефіцієнта ідеальності [1-4]. Питомі опори плівок ZnO, розраховані за лінійними відрізками вольт-амперних кривих.

Ключові слова: *оксид цинку (ZnO); термічне окислення; гетеропереходні діоди; оптоелектронні застосування; нанокристалічна структура; оптична заборонена зона; електричні властивості; вольт-амперні (ВАХ); температура підкладки; спектри фотолюмінесценції*